Synoptic-Scale Controls on the Sea Breeze of the Central New England Coast

SAMUEL T. K. MILLER

Department of Earth Sciences and Climate Change Research Center, Institute for the Study of Earth, Oceans and Space, University of New Hampshire, Durham, New Hampshire

BARRY D. KEIM

Department of Geography and Climate Change Research Center, Institute for the Study of Earth, Oceans and Space, University of New Hampshire, Durham, New Hampshire

(Manuscript received 9 April 2002, in final form 31 July 2002)

ABSTRACT

Using routinely available hourly surface observations and United States surface analyses for 2001, a method was developed for predicting sea-breeze events. The method is adaptable to any coastal region in the world where surface data are available. Specific prediction guidelines have been developed using Portsmouth, New Hampshire, as the forecast site. Using Portsmouth METARs (translated roughly from the French as aviation routine weather report), 167 days were determined to have conditions favorable for the occurrence of a sea breeze. Each of these 167 days are classified as either sea-breeze, marginal, or non-sea-breeze events. Sea breezes were defined as insolation-driven local onshore winds. Marginal events were weak sea breezes. Non-sea-breeze events were those days on which sufficient insolation was present but failed to produce a sea breeze at Portsmouth. The surface analyses for these 167 days were used to define a set of synoptic classes based on the arrangement of large-scale pressure systems, and meaningful interpretations resulted. For example, sea breezes and marginals account for almost 80% of one class, whereas two other classes produced no sea-breeze events. Standard surface observations were used to calculate the "regional scale" cross-shore potential temperature gradient ($\delta\theta/\delta x$) and the cross-shore geostrophic wind component (u_G) for the hour of onset (sea breeze and marginal events) or of peak heating (non-sea-breeze events). Stronger negative $\delta\theta/\delta x$ values were needed to develop a sea breeze in the presence of stronger positive u_G values. The six well-defined synoptic classes were plotted as a function of $\delta\theta/\delta x$ and u_G and occupy specific regions of the resulting diagram.

1. Introduction

The sea breeze is an important influence on New England's weather, climate, and air quality. The associated moisture can be responsible for creating fog near dawn, and for fueling afternoon convection at points well inland of the coast. Furthermore, the thermal internal boundary layer (TIBL) that forms within the marine air mass often traps pollutants in a shallow layer near the earth's surface, reducing air quality in the coastal zone (Hsu 1988). In New England, sea breezes have been shown to foster high tropospheric ozone (Gaza 1998; Seaman and Michelson 2000) and high sulfur dioxide episodes (Barbato 1975). For these reasons it would be useful to understand the meteorological conditions conducive to sea-breeze development in New England, and how these conditions vary with the synoptic-scale meteorological situation.

Corresponding author address: Dr. Sam Miller, Climate Change Research Center, University of New Hampshire, Morse Hall, Durham, NH 03824.
E-mail: stm@cisunix.unh.edu

Research on the New England sea breeze was carried out as part of the Atmospheric Investigation, Regional Modeling, Analysis, and Prediction (AIRMAP) project. AIRMAP's goal is to understand factors influencing New England's climate and air quality. The goal of the Central New England Seabreeze Study is to understand (and therefore be able to predict) the physical behavior of the sea breeze on the central New England coast, including its inland extent, vertical depth, and frontal characteristics. This paper focuses on the synoptic-scale surface environment in which the sea breeze develops. Future research will examine the meso- and microscale behavior of specific sea-breeze events under varying synoptic-scale conditions at different times of the year.

2. Pertinent literature

Some of the early work with New England sea breezes was carried out by Craig et al. (1945). They used psychrometric data recorded by balloons and aircraft along an east–west transect in Massachusetts Bay, and were able to document the characteristic raised-head wave structure later shown in much greater detail by Simpson

(1994, 1997). Fisher (1960) used vertical profiles along a cross-shore transect near Block Island, Rhode Island, to document the rotation of sea breezes by the Coriolis force. The Coriolis-induced rotation was later studied analytically by Neumann (1977). Frizolla and Fisher (1963) used pilot balloons to study sea breezes in the New York City area, finding that the opposing (continental) flow caused the leading edge of sea breezes to take on frontal characteristics, and that the associated marine air mass was shallower in events with stronger opposing winds. Simpson and Linden (1989) showed that frontogenesis was a general feature in horizontal density currents such as sea breezes, and a number of subsequent studies (e.g., Kraus et al. 1990; Reible et al. 1993) specifically examined sea-breeze frontogenesis. All of the latter studies referenced earlier theoretical work by Miller (1948).

Perhaps the most comprehensive observational study of sea breezes in New England was completed by Barbato (1975), who focused on forty 1972 sea-breeze events in the Boston, Massachusetts, area. Barbato determined that sea breezes penetrated as far as 29 km inland but were usually restricted to the bowl-shaped Boston basin region closer to the coastal zone. Using radiosonde data from eight sea-breeze events, it was found that the marine air mass varied in depth from 330 to 2230 m. He also found that sea-breeze events often significantly reduced air quality, particularly with respect to sulfur dioxide (SO_2).

Gaza (1998) identified the sea breeze as an important factor in a July 1995 tropospheric ozone (O_3) pollution event in southern New England and New York State. Pignotti (1987) identified the Appalachian leeside trough (APLT) as a contributor to high ozone concentrations in the northeastern United States, and Seaman and Michelson (2000) discussed the interaction of the APLT, the sea breeze, and several synoptic-scale features during high ozone events documented in North American Research Strategy for Tropospheric Ozone (NARSTO)-Northeast 1995 (U.S. EPA 1994).

The Kennedy Space Center, in east-central Florida, has also been the site of numerous sea-breeze studies. Of interest to this work are the numerical studies carried out by Zhong and Takle (1993), who modeled the effects of large-scale (synoptic) wind flow on meso- and microscale aspects of the sea breeze. They grouped sea breezes into two types; the first corresponded to large-scale flow that was either perpendicular (eastward) or antiparallel (southward) to the east Florida coastline, and the second corresponded to large-scale flow that was either antiperpendicular (westward) or parallel (northward) to the east Florida coastline. The two general classes of sea breezes differed in many respects, including the associated maximum vertical velocities.

3. Methods

It would be particularly useful to identify days on which sea breezes occurred and to compare them with synoptically similar days when sea breezes did *not* occur. The comparison might include general groupings of the arrangement of synoptic-scale pressure systems in the Northeast, and the resulting cross-shore potential temperature gradients and cross-shore geostrophic wind components. The cross-shore potential temperature gradient is a measure of the density contrast driving the sea breeze, and the cross-shore surface geostrophic wind component is a measure of the synoptic-scale movement of mass that opposes the sea breeze's inland propagation. For this comparison to be possible, a relatively simple and accurate means of identifying the dates of sea-breeze events is needed.

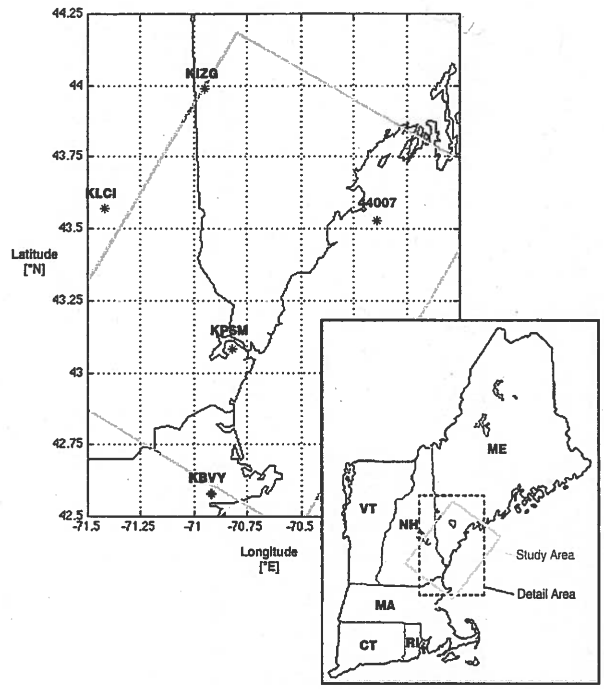

Fig. 1. Study area and location map. Gray line indicates edges of the study area. Surface weather observing stations shown are Fryeburg, ME (KIZG); the Portland, ME, buoy (44007); Portsmouth, NH (KPSM); Beverly, MA (KBVY); and Laconia, NH (KLCI).

Pease Air National Guard Base's (KPSM; see Fig. 1) weather observations were used to identify sea-breeze events. Pease is in Portsmouth, New Hampshire, and also happens to be in a relatively central location on the study area's coastline. It is equipped with top-of-the-line weather equipment and is operated 24 hours per day, 7 days per week, by a human weather observer—not an Automated Surface Observing System (ASOS). Because of these points, it was assumed that Pease's hourly observation records are satisfactory for identifying sea-breeze events throughout the study area's coastal zone. It was also assumed that the influences of the Great Bay, which surrounds Pease on two sides, and the Piscataqua River, to the north of the airfield, are small when compared with that of the Atlantic Ocean.

While the sea breeze is often easily identifiable by sharp wind, temperature, and humidity changes marking its arrival, experience in weather observation has shown that it is occasionally an ambiguous event. One kind of ambiguity is the initial occurrence of a southeasterly wind that has nothing to do with a sea breeze, to which a sea breeze is added later in the day. Other kinds of ambiguity are a very weak sea breeze developing late in the afternoon, or of very short duration, or lacking one or more of the defining characteristics noted above.

With this is mind, nomenclature for three different "event" definitions was developed:

1) A *sea-breeze event* occurs when the surface wind in the study area is from some direction other than the southeast at the beginning of the day, shifts to the southeast during midday, and then shifts to another direction in the evening. (Any wind between 95° and 174° is considered southeasterly, although the sea breeze at Pease generally comes from 130°.) The shift to a southeasterly wind must not be associated with a synoptic-scale pressure system. The observed sky conditions should be characterized by less than "broken" (BKN; 5/8 sky cover or more) cloud coverage in the low (surface to 1981 m above ground level) and middle (1981–7010 m) *etages,* on the assumptions that the local temperature contrast that drives the sea-breeze cell is powered by insolation, and that high-*etage* (higher than 5029 m) clouds are generally thin and do not significantly reduce insolation. [Sky cover contractions are defined in U.S. Air Force (1998); see WMO (1956) for cloud *etages.*]
2) A *non-sea-breeze event* is one in which the background conditions resemble those of a sea-breeze event, except that the daytime wind shift to the southeast does not occur.
3) A *marginal event* is one in which the sea breeze occurs at Portsmouth, but is very short lived (2 h or less), is marked by very light wind speeds, or merely manifests as a short interval of "light and variable" winds during a period of sustained wind from a nonsoutheasterly direction.

Days on which the wind was already from the southeast at sunrise were excluded from this study. While it seems likely that the sea breeze can supplement a synoptically driven southeasterly wind, it was decided to reserve this kind of event for later studies.

4. Event identification

The KPSM official Surface Weather Observations form was used to provisionally identify all sea-breeze, marginal, and non-sea-breeze events for the calendar year 2001 (January–December). Sea breezes and marginal events were identified using the following tests:

1) Surface wind at Pease was from the northwest, northeast, southwest, or "variable" (only if associated with "light" winds) for the majority of the early morning hours prior to the onset of the sea breeze. [Light winds are defined as "6 knots or less" in U.S. Air Force (1998).]
2) Wind direction changed to southeast (usually 130° true, but any direction between 95° and 174° was allowable) after onset, lasting more than 2 h. (Two hours or less was classified as a "marginal" event.) Sea-breeze-associated southeasterly winds were differentiated from synoptically driven southeasterly winds using the following criteria:
   a) Sea breezes manifest at Pease as either a "sudden" shift (occurring over a period of several minutes) in wind direction to the southeast, or as a prolonged transition from steady winds out of the synoptically driven wind direction (e.g., northwest), followed by a 1–2-h period of light and variable winds (speed less than 7 kt, possibly with direction reported as variable by the observer), then shifting to a steady southeasterly direction.
   b) Onshore winds not associated with sea breezes were identified as those where the wind direction gradually shifted to a southeasterly direction over a period of several hours, coincident with an observed sky condition (cloud cover) and/or other weather phenomena indicative of an approaching synoptic-scale system, such as shields of "invading" high cloud, systematically increasing middle-*etage* or low-*etage* clouds, or nonshowery precipitation. [See WMO (1956) for descriptions of low-, mid-, and high-*etage* clouds.]
3) The wind direction returned to northwest, northeast, southwest, or variable following the end of the sea-breeze event.
4) There was less than BKN cloud cover in both the low and middle *etages* prior to onset. This was chosen because the physical mechanism driving the sea breeze is insolation and differential surface heating in the coastal zone, and BKN or greater coverage in the low and middle *etages* was assumed to significantly reduce surface insolation. Total high cloud coverage was excluded because of the assumption that high clouds are generally thin and do not usually reduce insolation significantly.
5) There was no "significant" precipitation (one or two brief, light showers, encoded -SHRA, were permissible) within the 6-h period prior to onset of the sea breeze. [We relied on the observer's assigned intensity to identify "light" rainshowers; see U.S. Air Force (1998) for a precise description of how these intensities are assigned. "Brief" means "minutes rather than hours."] In the event that the southeasterly wind might have been synoptically driven by a fast-moving system that was undetected by the checks listed in criteria 1–4 above, significant precipitation prior to onset of the southeasterly wind could serve as an additional indication that it is not

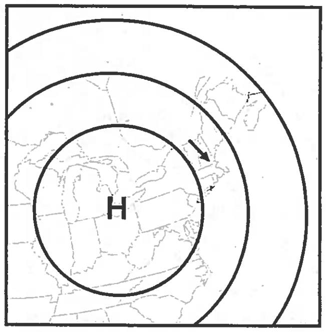

FIG. 2. Synoptic class 1. Westerly to northerly geostrophic wind with a large high (or open ridge) dominates the region. Surface isobars are anticyclonically curved.

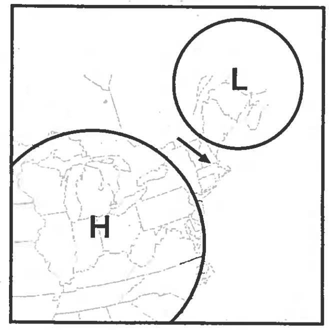

FIG. 3. Synoptic class 2. Westerly to northerly geostrophic wind with a weak high (or open ridge) shares dominance of the region with a weak low (or open trough). Surface isobars have no significant curvature.

necessarily associated with local-scale differential heating.

Once the sea-breeze and marginal events were provisionally identified from the KPSM observations, the National Weather Service (NWS) U.S. surface analyses charts for 1200 UTC (0700 LST) on these days were downloaded from either the National Virtual Data System (NVDS) Website (January–October; online at http://nndc.noaa.gov/?http://ols.ncdc.noaa.gov/cgi-bin/nndc/buyOL006.cgi?FNC=chart_Ancep_get_chart_htm) or the NWS fax ftp site (November and December; see ftp://weather.noaa.gov/fax/). These were then examined for the direction of the geostrophic wind in the study area. If the surface analysis for the event in question suggested that the southeasterly wind was caused by synoptic-scale circulation, the event was removed from consideration altogether, that is, not classified as a sea-breeze, marginal, or non-sea-breeze (see below) event.

"Non-sea-breeze" events were identified using tests 1, 4, and 5 above. Surface analyses for 1200 UTC on these days were also downloaded from either the NVDS Web site or the NWS ftp site. If the event "passed" the sea-breeze tests outlined in tests 1, 4, and 5, but no sea breeze occurred, it was classified as a non-sea-breeze event.

A total of 59 sea-breeze events, 10 marginal events, and 98 non-sea-breeze events were identified. (For a complete list of these, see http://www.ccrc.sr.unh.edu/~stm/AS/Research/2001_Events.html.)

5. Definition of synoptic classes

Zhong and Takle (1993), among others, demonstrate that the arrangement of synoptic-scale features, and the resulting geostrophic wind, are important controls on sea-breeze behavior. For example, a synoptically driven northwesterly wind would probably cause very different sea-breeze behavior in our study area (Fig. 1) than would a shore-parallel southwesterly wind.

The 1200 UTC surface charts for the 167 sea-breeze-favorable days were parsed according to the general direction of the geostrophic wind over the study area, as implied by surface isobars:

- group A—northwesterly (271°–360° true), that is, having a significant component perpendicular to the coastline;
- group B—southwesterly (180°–270° true), that is, the largest component of the wind is parallel to the coastline;
- group C—northeasterly (001°–090° true), that is, the largest component of the wind is antiparallel to the coastline.

Any days with synoptic-scale geostrophic winds from the southeast quadrant would have by definition been excluded from the analysis (see above), though no cases occurred.

A second screening was made that further refined groups A and B. This led to three subcategories for the group A cases (total of 93), called classes 1, 2, and 3:

- Class 1 (Fig. 2)—An areally large, well-defined high pressure cell is generally located somewhere to the west of the study area. The curvature of the isobars over the study area is anticyclonic, meaning that the lower atmosphere is dynamically stable (25 cases).
- Class 2 (Fig. 3)—A somewhat weaker high pressure cell (or open surface ridge) is generally to the south or west of the study area, and a weak low pressure area (cell or trough) is to the north or east. Neither system dominates, and the resulting isobaric curvature is either very slight or neutral (51 cases).
- Class 3 (Fig. 4)—A strong low pressure cell is located to the northeast and dominates the study area. The surface isobars are cyclonically curved, meaning that the lower atmosphere is dynamically unstable (17 cases).

All three of these classes resulted in a northwesterly geostrophic wind in the study area. Group B (38 cases) was subdivided into two smaller groups, called classes 4 and 5:

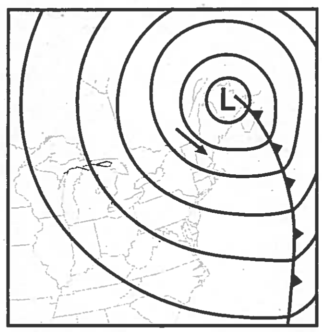

FIG. 4. Synoptic class 3. Westerly to northerly geostrophic wind with a large low dominates the region. Surface isobars are cyclonically curved.

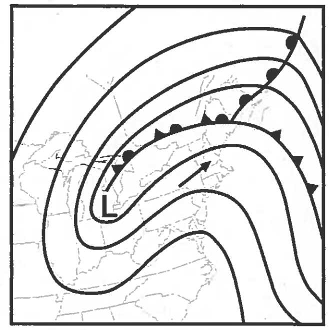

FIG. 6. Synoptic class 5. Postfrontal southerly to westerly geostrophic wind, with a low with associated trough (or front) to the west, a weak ridge immediately to the east, and a front farther east.

Class 4 (Fig. 5)—A large high pressure cell is located in the southeastern United States, and a low is located either in the upper midwest, Great Lakes, or the southern Hudson Bay region, with or without a front extending into the central part of the United States. The isobars over the study area are either anticyclonically or cyclonically curved, but the former tends to dominate. This class includes two situations that are similar in appearance on a surface chart but are dynamically very different. These are described in section 6 (31 cases).

Class 5 (Fig. 6)—A southwesterly geostrophic wind follows the passage of a mature frontal system, with a low to the west of the study area and a weak ridge immediately to the east (and immediately behind a cold or occluded front) (seven cases).

Group C, renamed class 6 for consistency, tends to be fairly uniform in terms of the arrangement of synoptic features and is not further subdivided. In general, synoptic class 6 (Fig. 7) is associated with a high (or northeastward-tilting ridge) to the northwest and a low (or frontal system) to the southeast of the study area (31 cases).

There were five cases that did not fit any of the above classes, and these were grouped together into class 7—miscellaneous. No further breakdown was made of this class.

Table 1 summarizes the occurrences of the synoptic classes and their associated percentages of the total. Figures 2–7 illustrate the general configuration of surface synoptic pressure systems associated with each class.

6. Synoptic classes associated with sea-breeze, marginal, and non-sea-breeze events

The occurrences of the sea-breeze, marginal, and non-sea-breeze events were compared to the synoptic classes described in Figs. 2–7 (Table 2). A χ^2 calculation indicates rejecting the null hypothesis ($p < 0.05$). Rejecting the null hypothesis indicates that the distribution of events in the table is nonrandom and is, therefore, associated with synoptic class. [For more about the χ^2, see Johnson (1992) or Clark and Hosking (1986).]

The sea-breeze–non-sea-breeze event distribution evolves gradually over the first three classes. Out of the 25 class 1 cases, 60% resulted in the occurrence of a sea breeze. Class 2 (the largest of the seven) is distributed between sea breezes, marginals, and non–sea breezes, with non–sea breezes dominating (76%). Class 3 cases are exclusively associated with non–sea breezes.

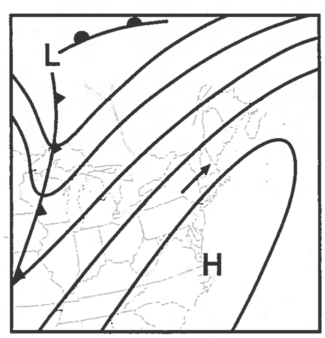

FIG. 5. Synoptic class 4. Prefrontal southerly to westerly geostrophic wind with a high (or open ridge) located south of the study area, and a low with associated trough (or front) to the west. This class also includes the circumstance in which the isobar closest to the high center in the southeast does not wrap back around the eastern side of the high. (See text for additional details.)

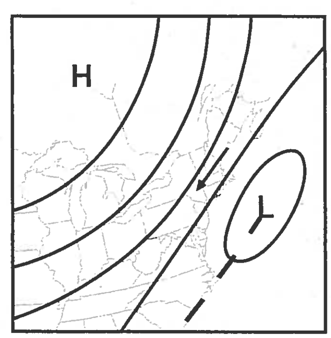

FIG. 7. Synoptic class 6. Northerly to easterly geostrophic wind with a high (or northeastward-tilting open ridge) located to the northwest, and a low (or open trough) to the southeast.

TABLE 1. Occurrences of synoptic classes and associated percentages of all occurrences.

Group	Synoptic class	No. of cases	Percentage of total
A	1	25	15.0
	2	51	30.5
	3	17	10.2
	1, 2, and 3 combined	93	55.7
B	4	31	18.6
	5	7	4.2
	4 and 5 combined	38	22.8
C	6	31	18.6
Miscellaneous	7	5	3.0
	All	167	

TABLE 2. Comparison of sea-breeze, marginal, and non-sea-breeze events with synoptic classes.

Synoptic class	Sea-breeze events	Marginal events	Non-sea-breeze events	All events
1	15	2	8	25
2	9	3	39	51
3	0	0	17	17
4	12	2	17	31
5	0	0	7	7
6	21	3	7	31
7	2	0	3	5

We speculate that this distribution arises from a combination of the cross-shore geostrophic wind component (u_G) and the magnitude of the cold-air advection associated with the low-level flow. Large values of either are likely to prevent a sea breeze. (This is examined in somewhat more detail below.)

If marginal events are grouped with sea-breeze events, the distribution is almost evenly divided in class 4. We speculate that the reason for this bifurcation is that class 4 includes two situations that are superficially similar in appearance, but quite different in origin. In the first situation, the high to the south of New England is a migratory anticyclone associated with a modified continental polar air mass. (Southwesterly flow in the study area precedes the passage of a frontal system.) In the second situation, the high is an extension of the semipermanent subtropical ridge, and is associated with a maritime tropical air mass. (Southwesterly winds in the study area result from the flow around the western extent of the Bermuda high.) The cross-shore temperature gradient, and therefore the density contrast that drives the sea breeze in the study area, would be different in these two situations. In the former, cool, dry air would be on the land side, and—given a relatively cool sea surface temperature—the land–sea temperature gradient would be weak. In the latter, warm, moist air would be on the land side, and the driving force for a sea breeze would be strong.

As with class 3, class 5 is exclusively non–sea breeze. Once again, this distribution probably arises from the magnitude of u_G and cross-shore cold-air advection associated with the synoptic-scale systems. Almost 70% of class 6 cases (21 of 31 total cases) are sea-breeze events, with the remaining 30% distributed among the marginal and non-sea-breeze events. The class 7 cases probably do not represent any meaningful physical information, as this is a miscellaneous category.

7. "Regional scale" temperature gradients and geostrophic wind

To explain the distribution of synoptic-scale forcing and sea-breeze events described above, the cross-shore potential temperature gradient ($\delta\theta/\delta x$) that gives rise to the sea breeze was compared to the cross-shore geostrophic wind component (u_G) that resists the inland penetration of the sea breeze. This method is similar to one developed by Simpson (1994, chapter 4) for Thorney Island, in the United Kingdom.

Regional-scale calculations were completed for all 167 events, using reported sea level equivalent pressures (SLPs) and air temperatures reported by four widely separated stations (Fig. 1). The four stations were chosen to represent the thermal and pressure forcing near the edges of "the box" defining the study area in the north–south and east–west directions. It was assumed that the Fryeburg–Beverly (KIZG–KBVY) differences sufficiently represented the north–south gradients, and the Portland–Laconia (44007–KLCI) differences sufficiently represented the east–west gradients.

Sea level pressures and the mean latitude of the four stations (43.4175°N) were used to calculate the two components of the geostrophic wind. Reported air temperatures were converted to potential temperatures using station elevations and an exponential vertical pressure function (to estimate the station pressure from SLP), then the potential temperature gradients were estimated using first-order finite differences (Carnahan et al. 1990). These gradients were deliberately estimated using a linear method and could, no doubt, be improved with more sophisticated techniques. Equivalent geostrophic wind and potential temperature gradient components were then determined for a coordinate system rotated $-30°$. This rotation was introduced because the coastline in the study area, if estimated by a straight line, is approximately 30° clockwise from north. Rotating the vector components results in a cross-shore component x' that points toward 120° true and an alongshore component y' that points toward 30° true. The result was a set of regional-scale cross-shore and alongshore geostrophic wind (u_G, v_G) and potential temperature gradients ($\delta\theta/\delta x$, $\delta\theta/\delta y$).

The date and synoptic class associated with each event were cross-referenced with $\delta\theta/\delta x$ and u_G (the cross-shore components) for either the hour closest to the onset of the event (for sea breeze and marginals) or 1400 LST (for non-sea-breeze events). The choice of 1400 LST was made for the latter group because this

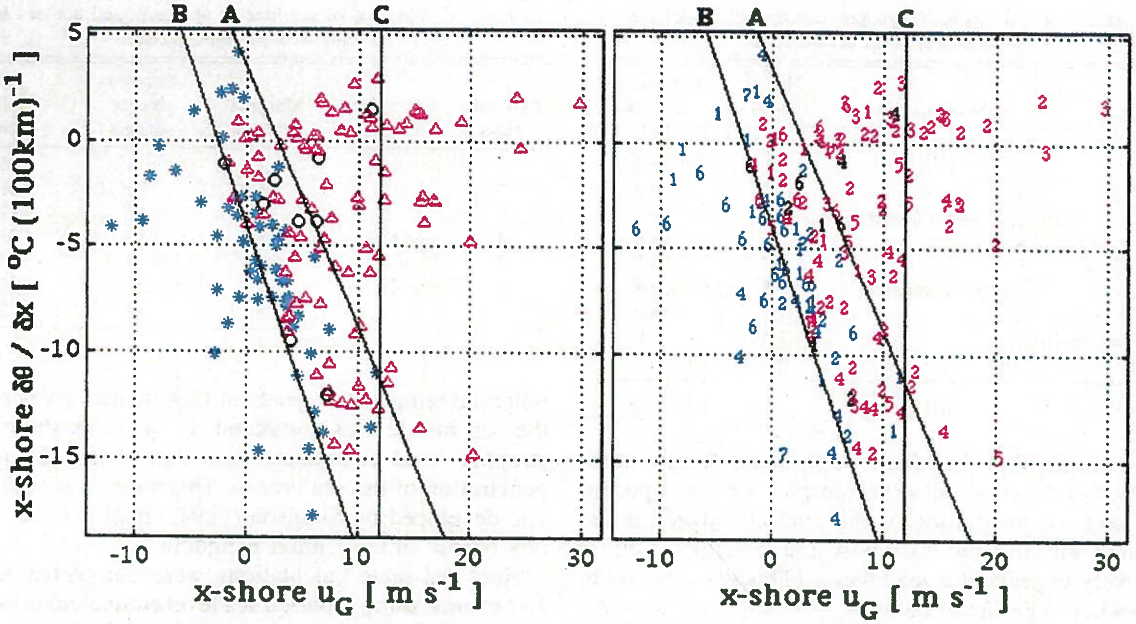

FIG. 8. (left) All sea-breeze, marginal, and non-sea-breeze events as a function of their associated cross-shore regional-scale potential temperature gradients and geostrophic wind components. Events are plotted using the regional-scale temperature gradients and geostrophic wind components present at either the time of onset (for sea breeze and marginals), or 1400 LST (for non–sea-breezes). Sea-breeze events are depicted with a blue star (*), marginal events with a black circle (○), and non–sea breezes with a red delta (Δ). (right) Synoptic classes of sea-breeze, marginal, and non-sea-breeze events. Sea-breeze events are depicted with blue text, marginal events with black text, and non–sea breezes with red text.

approximately coincides with the time of peak surface heating and maximum diurnal land–sea temperature contrast. Figures 8–14 illustrate results of these comparisons.

a. General discussion

Figure 8 shows that it takes stronger $\delta\theta/\delta x$ to overcome stronger u_G, and initiate a sea breeze detectable

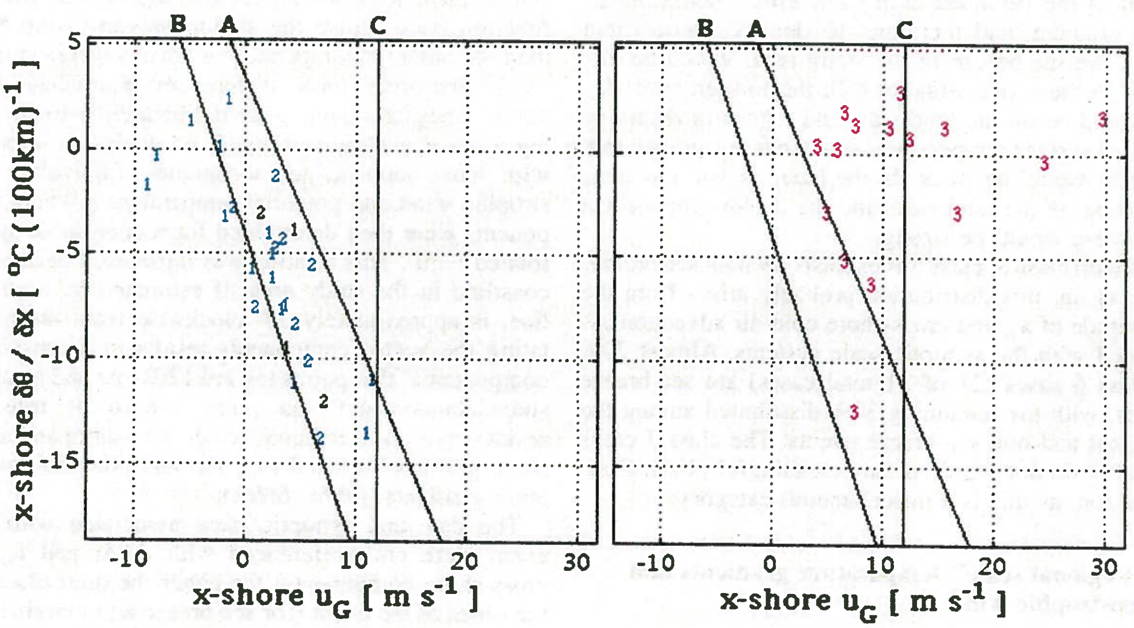

FIG. 9. (left) Sea-breeze and marginal events associated with class 1 and class 2 cases. (right) Non-sea-breeze events associated with class 3 cases. Axes and color coding of events are as described for Fig. 8.

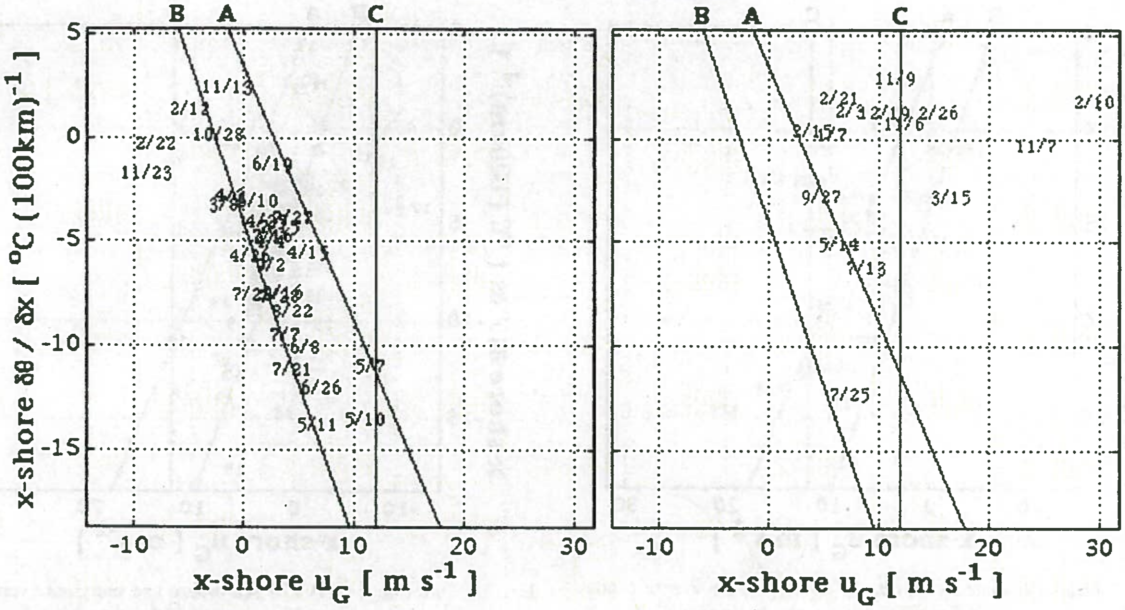

FIG. 10. (left) Dates of sea-breeze and marginal events associated with class 1 and class 2 cases. Date format is month/day. (right) Dates of non-sea-breeze events associated with class 3 cases. Axes are as described for the above figures.

at Pease. Line A shows the critical limits that are needed for both independent variables to prevent a sea breeze from overcoming an opposing synoptically driven wind. In the region above or to the right of A, $\delta\theta/\delta x$ is too weak to overcome the opposing u_G. Line B defines the critical limits below which a sea breeze will always occur. In the region below or to the left of B, u_G is either *onshore* or too weak to prevent $\delta\theta/\delta x$ from initiating a sea breeze. Most of the marginal events (with three exceptions) lie in the crossover region between A and B. Line C defines what appears to be a cutoff value in the geostrophic wind: no seabreeze events occurred with u_G greater than about 12 m s^{-1}, or 25 kt.

Note that along line A, u_G is 3 m s^{-1} where $\delta\theta/\delta x$ is zero. This indicates that, in the absence of a favorable regional-scale cross-shore potential temperature contrast, the sea breeze can still overcome a "light" opposing wind (as defined in U.S. Air Force 1998). A

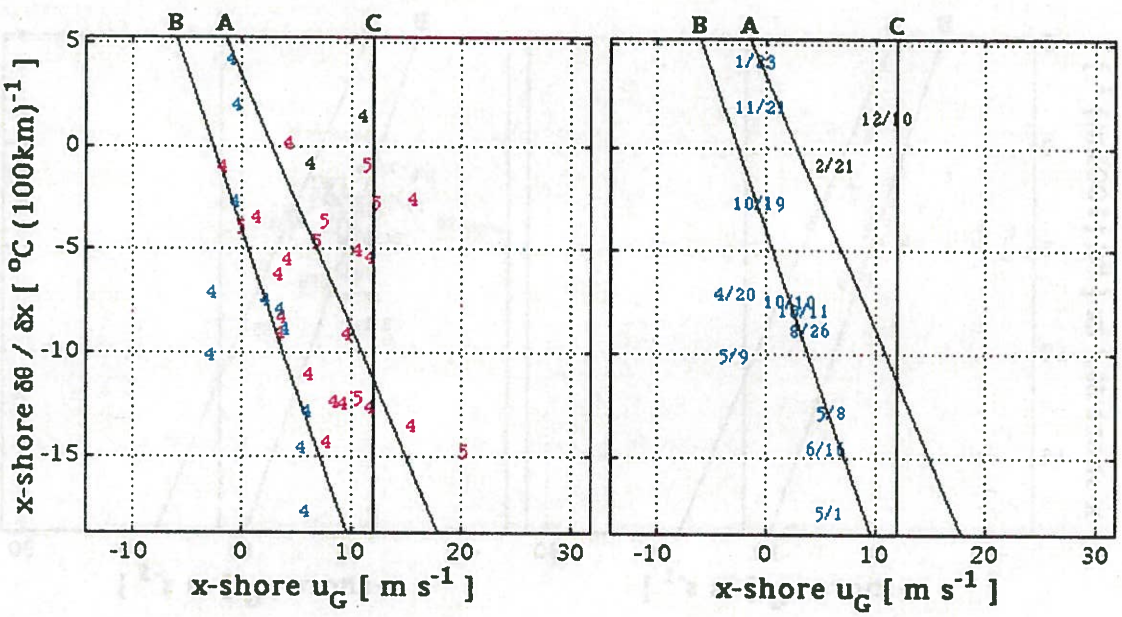

FIG. 11. (left) All events associated with class 4 and 5 cases, by synoptic class. (right) Dates associated with class 4 sea-breeze and marginal events. Axes and color coding of events are as described for the above figures.

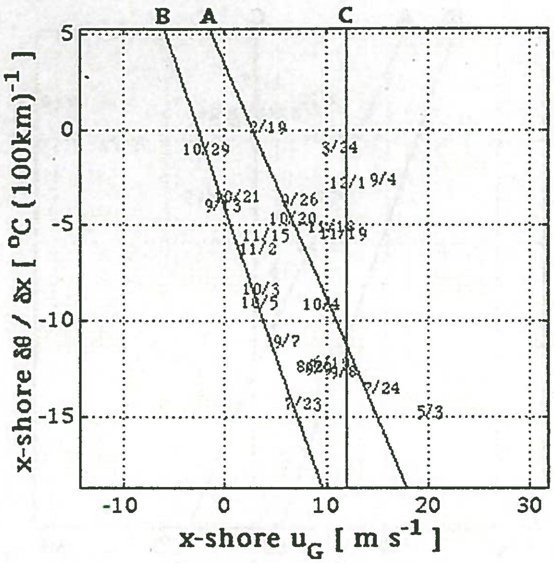

FIG. 12. Dates associated with class 4 and 5 non-sea-breeze events. Axes are as described for the above figures.

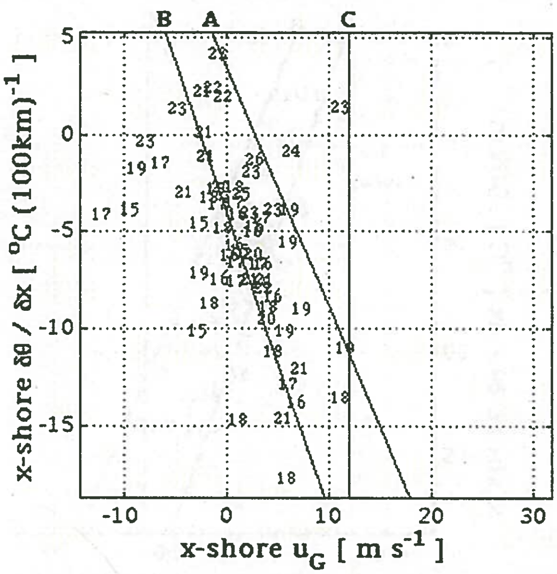

FIG. 14. Onset hour (UTC) of sea-breeze and marginal events, all synoptic classes. Axes are as described for the above figures.

related observation is that sea-breeze events can occur even if $\delta\theta/\delta x$ is in the wrong direction, that is, indicating warmer air offshore rather than on land. We speculate that, under certain circumstances, favorable cross-shore temperature gradients develop in the immediate coastal zone that are not detected by this regional-scale calculation.

Figure 8 (right-hand panel) also shows the synoptic classes associated with the sea-breeze, marginal, and non-sea-breeze events. Beginning with the lower left, it is apparent that the strongest sea breezes are associated with synoptic classes 4 and 6. This is entirely reasonable given that these two were initially defined as situations where the isobars indicated a relatively weak u_G. In the upper-right corner, one finds that the strongest non-sea-breeze events are mostly associated with synoptic classes 2 and 3, with class 3 marking the extreme limit. Once again, this is reasonable because class 3 was defined as a scenario where the study area is dominated by northwesterly winds on the cold side of an intense low pressure system. Such a location is subject to very strong northwesterly winds and strong cold-air advec-

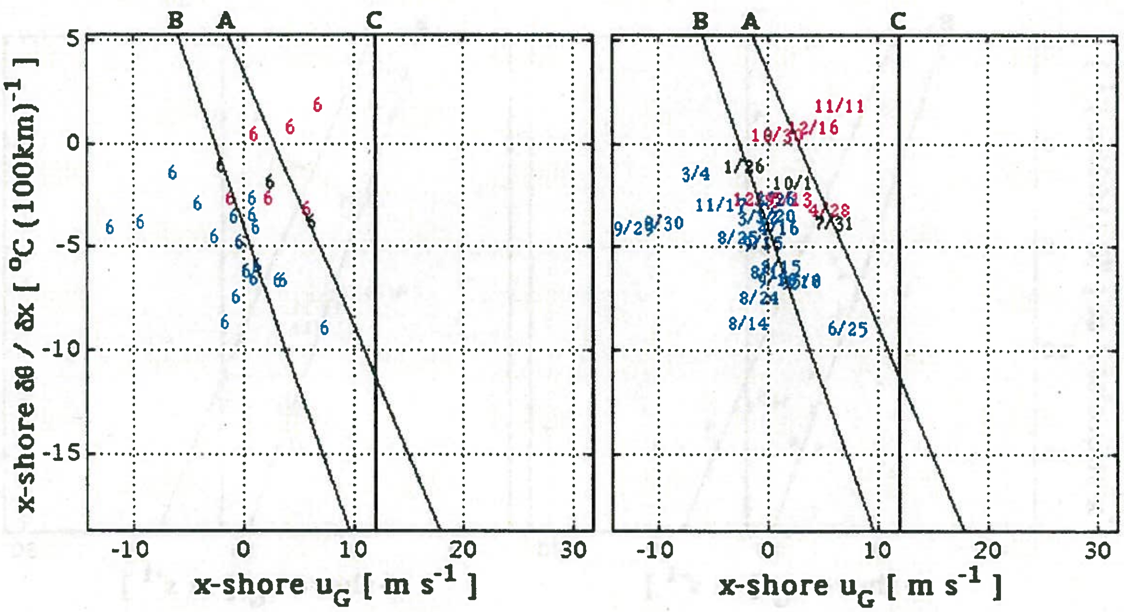

FIG. 13. (left) All sea-breeze, marginal, and non-sea-breeze events associated with class 6. (right) Dates of class 6 sea-breeze, marginal, and non-sea-breeze events. Axes and color coding of events are as described for the above figures.

tion, neither of which are conducive to the formation of a sea breeze. Similar arguments hold for the scenario defining class 2.

b. Classes 1, 2, and 3

Figure 9 (left-hand panel) shows that most of the sea-breeze and marginal events associated with synoptic classes 1 and 2 lie within the crossover region between lines A and B. Very few occur to the left side of the diagram, where u_G is -5 m s^{-1} or less, and none of them reach as far toward the lower-left corner as do the class-4- and -6-associated sea-breeze events noted in Fig. 8. Because of the associated $\delta\theta/\delta x$ and u_G values, class-1- and -2-associated sea-breeze events should range from slow-moving, thermally strong systems (bottom center) to relatively fast-moving, thermally weak systems (upper left). The large span of these three synoptic classes on the $\delta\theta/\delta x$ axis indicates that these classes, and their associated sea-breeze and marginal events, can occur over a very wide range of temperature regimes and, therefore, over a wide seasonal range.

Non-sea-breeze events extend in a triangle-shaped region from the left edge of the crossover region to the upper-right corner of the diagram, indicating that the highest values of u_G are associated with positive $\delta\theta/\delta x$, that is, with colder air over land and warmer air over the sea surface, and therefore are not favorable for the formation of a sea breeze. Figure 9 (right-hand panel) shows that most of the class 3 cases (all associated with non-sea-breeze events) occur in the upper-right quadrant of the diagram, where the temperature gradient and geostrophic wind conditions are least favorable for sea-breeze formation. One would expect that the class 3 cases would primarily occur during winter, when the long-wave trough and polar jet over the eastern half of the country have a high amplitude, rendering the New England region subject to the passage of intense baroclinic cyclones.

Figure 10 (left-hand panel) shows the dates associated with sea-breeze and marginal events coincident with synoptic classes 1 and 2. Note that the dates span the calendar from mid-February through late November. A seasonal pattern also emerges, with most summer events appearing in the lower half of the diagram—in the region of highly favorable $\delta\theta/\delta x$—and all of "nonsummer" events appearing in the upper half—in the region of weak or reversed $\delta\theta/\delta x$. This indicates that, in general, sea breezes can occur with larger opposing u_G in summer than during other seasons. Of particular interest are two February events, one October event, and one November event toward the upper left, with unfavorable $\delta\theta/\delta x$ values, but weak to negative u_G values. There are (at least) two possible explanations for this: 1) these events were mischaracterized as sea-breeze events or 2) the sea breezes were driven by local-scale temperature gradients that were too small (confined within a narrow zone immediately adjacent to the shoreline) to register in the regional-scale calculation used here. The second possibility will be examined in subsequent research.

Figure 10 (right-hand panel) shows the dates associated with the synoptic class 3 cases—all non-sea-breeze events. As expected, those cases occurring during winter are located near the upper boundary of the diagram, where $\delta\theta/\delta x$ is weak or unfavorable, that is, where the sea surface temperature is the same as or warmer than land. More than half of the class 3 cases occurred in November–February, and the strongest non-sea-breeze event, located near the upper-right corner (where a strong positive u_G opposes the sea breeze), occurred on 10 February.

c. Classes 4 and 5

Of all the synoptic classes, class 4 cases have the widest range of $\delta\theta/\delta x$ (Fig. 11). This probably reflects the wide annual range over which this class occurs, as well as the two superficially similar but dynamically different scenarios included in class 4 (described above). With the largest part of the geostrophic wind vector parallel (rather than perpendicular, by definition) to the coastline, the sea-breeze and marginal events occur farther toward the lower-left corner than do the same types of events associated with classes 1 and 2. Values of u_G for all types of events are generally biased further toward the negative than are those associated with classes 1–3. The u_G overlap between sea-breeze and non-sea-breeze events essentially disappears toward the lower boundary of the diagram, where $\delta\theta/\delta x$ is most favorable, but becomes more pronounced nearer the middle region and upper boundary of the diagram, where $\delta\theta/\delta x$ is less favorable for a sea breeze. This means that forecasting the occurrence/nonoccurrence of the sea breeze in the lower half of the diagram is a straightforward endeavor, but is somewhat more uncertain toward the upper half. The former cases (where $\delta\theta/\delta x$ is most favorable) are probably associated with the semipermanent Bermuda high and maritime tropical air mass in the southeast United States, and the latter cases (where $\delta\theta/\delta x$ is less favorable) are probably associated with migratory anticyclones and modified continental polar air masses.

Sea-breeze and marginal events associated with class 4 span a wide range of $\delta\theta/\delta x$ values, and they tend to cluster closer to the lower boundary than the upper, where $\delta\theta/\delta x$ values are more favorable. (See Fig. 11.) All of the sea-breeze and marginal cases are clustered between u_G values of -3 and $+12$ m s^{-1}. Some remnant of the (diagonal) marginal crossover region remains, although the region is somewhat more vertical in this coordinate system, because of the assumptions defining class 4 (wind parallel to the coast), which force the sea-breeze event region into a more vertical position. Note also that there are no sea-breeze or marginal events associated with class 5 cases.

Figure 11 (right-hand panel) shows the dates associated with class 4 sea-breeze and marginal events. A general picture emerges that is similar to the class 1–3 picture, with summer events appearing nearer the lower boundary of the diagram and nonsummer events appearing nearer the upper boundary. Of particular interest is the 23 January sea-breeze event near the upper boundary. This event is associated with an unfavorable $\delta\theta/\delta x$, but an essentially nonexistent opposing u_G. It is likely that an extremely narrow band of warm surface temperatures developed on the coastal plain immediately adjacent to the shore. A very narrow band of relatively warm air on the land side of the coast is not conducive to "strong" sea breezes, as any landward intrusion of the marine air mass would quickly extinguish the favorable $\delta\theta/\delta x$ and shut down the driving force.

Figure 12 shows the dates associated with class 4 and 5 non-sea-breeze events. The seasonal pattern described above is again evident, with the exception of several midautumn events near the center of the diagram. It is not surprising that several non-sea-breeze events occur toward the lower half of the diagram. During late summer and early autumn, the warmest conditions along the central New England coast occur with a southwesterly wind, when warm air is advected from the southern United States and the Gulf of Mexico. This sets up warmer air temperatures on the land side of the coast. There are two mechanisms responsible for cooling the surface waters of the Gulf of Maine in late autumn, and thus setting up the cooler air temperatures on the seaside of the coast: local heat loss due to vertical heat fluxes (Brown and Irish 1993; Miller 1999) and Ekman pumping. The former begins to take effect in early October. The latter occurs anytime there is a southwesterly surface wind along the coast, which sets up surface Ekman transport toward the east, and net ocean mass transport toward the southeast (Apel 1987). Surface flow away from the coast, coupled with mass conservation, forces upwelling in the coastal zone, and upwelling brings cooler water to the ocean surface (Feng 1996). The combination of southwesterly warm-air advection over land and cool sea surface temperatures places the $\delta\theta/\delta x$ in a sea-breeze-favorable range, but the sea breeze is prevented from reaching Pease because of the relatively strong southwesterly winds.

d. Class 6

Like the class-1-, -2-, and -3-related sea-breeze events, synoptic class 6 sea-breeze events seem to occupy a fairly coherent region of the diagram (Fig. 13), but the crossover area between sea breezes and non–sea breezes is narrower than it is for the former events. A forecaster can therefore use the diagram to predict sea-breeze events in class 6 cases with a high degree of confidence.

Ignoring the marginals and the non–sea breezes, late summer/early fall appear to cluster toward the lower left of the class 6 grouping (where u_G is onshore), winter and late fall toward the upper boundary (where $\delta\theta/\delta x$ is least favorable), and summer toward the center of the diagram (where $\delta\theta/\delta x$ is more favorable) (Fig. 13, right-hand panel). The latter two observations are relatively simple to explain with the expected seasonal variations. The first of the three observations may be an artifact of the relatively small sample (31 cases spread out over a single year), and two objectives of future work should be to increase the total number of cases observed, and to extend the database of events from one to several years.

e. Hour of onset

Figure 14 shows the hour (UTC) closest to the time of onset of the sea breeze at Pease, as best as could be determined using the KPSM observations. Hours that are greater than 24 correspond to the early UTC hours of the following day: subtract 24 to convert to a 24-h clock. The conversion from UTC to local standard time (LST) is −5. (For example, "26" should be understood as "02" UTC, or 2100 LST.)

Sea-breeze events near the top left of the diagram occur relatively late in the day, which is not surprising, since this is a region on the diagram where the land–sea temperature forcing is weak, and a sea breeze is only possible when the opposing u_G is weak. There are three cases in this region where the sea breeze did not arrive at Pease until 2300 UTC, or 1800 LST. Toward the bottom center of the diagram, where $\delta\theta/\delta x$ is highly favorable and the opposition from u_G is still relatively weak, the latest onset time is 2100 UTC (1600 LST) with 1800 UTC (1300 LST) more common, and one case as early as 1600 UTC (1100 LST).

Some, but not all, of the earliest onset times occur toward the lower left, where both $\delta\theta/\delta x$ and u_G are favorable. Some of these cases are those with onset times as early as 1500 UTC (1000 LST). But there are other events with equally early onset times in the crossover region, toward the center of the diagram. All of the marginal events occur at 1900 UTC (1400 LST) or later, although there are definite sea-breeze events that begin later than the latest marginal event.

In short, while there appears to be some weak tendencies toward 1) later onset periods for marginals than for sea-breeze events; 2) later onsets toward the upper left (where $\delta\theta/\delta x$ is either very weak or unfavorable) than toward the bottom center; and 3) earlier onsets toward the lower left (where $\delta\theta/\delta x$ and u_G are both highly favorable), these are fairly weak tendencies and can hardly be considered conclusive. It appears that the one-way "strong ⇒ early" formulation is valid from this diagram, but proving the two-way formulation will require looking at an average onset time over the entire 120-km-long coastline in the study area. These results suggest that this generally unclear picture would arise if the sea breeze were nonhomogeneous in the alongshore direction.

8. Summary and conclusions

Using routinely available hourly surface observations and United States surface analyses for the year 2001, a method was developed for predicting sea-breeze events. The method is adaptable to any coastal region in the world where surface data are available. We developed specific prediction guidelines using Portsmouth, New Hampshire, as the forecast site.

Using the Pease Air National Guard Base (in Portsmouth, New Hampshire) weather observation records, 167 days in 2001 were identified that had conditions favorable for the formation of a sea breeze on the central New England coastline. Favorable conditions were defined as the absence of significant cloud cover in the low and middle *etages,* and the nonoccurrence of significant precipitation, thereby permitting insolation to establish a cross-shore potential temperature gradient. Days when synoptic-scale forcing was responsible for onshore flow were excluded from the study. These 167 days were grouped into sea-breeze, marginal, and non-sea-breeze events. Sea-breeze events were those days on which the wind direction shifted from southwest, northwest, or northeast to southeast during midday and then back to southwest, northwest, or northeast in the evening. Non-sea-breeze events were those days on which the wind shift did not occur, in spite of relatively cloud-free skies. Marginal events were those days on which the sea breeze occurred, but was short lived (lasting 2 h or less) or exceptionally weak (characterized by very light wind speeds, with or without a highly variable wind direction). A total of 59 sea-breeze events, 10 marginal events, and 98 non-sea-breeze events were identified for 2001.

The 1200 UTC surface synoptic situations for all 167 event days were evaluated using NWS United States surface analyses. These situations were grouped into seven different general classes, where classes 1, 2, and 3 corresponded to northwesterly geostrophic winds, classes 4 and 5 corresponded to southwesterly winds, and class 6 corresponded to northeasterly winds over the study area. Class 7 was a miscellaneous grouping. We found that sea breezes occurred about 60% of the time with class 1, about 20% of the time with class 2, and never with class 3. Sea-breeze or marginal events were almost as likely as non–sea breezes with class 4, but never occurred with class 5. Sea-breeze and marginal events accounted for almost 80% of the class 6 cases.

Four stations—one each near the northern, eastern, southern, and western boundaries of the study area—were used to calculate "regional scale" cross-shore potential temperature gradients ($\delta\theta/\delta x$) and cross-shore geostrophic wind components (u_G). The former is a measure of the force driving the sea breeze, and the latter is a measure of the force opposing the sea breeze. A diagram was set up with u_G on the horizontal axis and $\delta\theta/\delta x$ on the vertical axis. Synoptic classes and the dates of all three types of events were plotted on these axes, as well as the hour of onset for sea-breeze and marginal events. (See Figs. 8–14.)

In general, it was found that stronger negative $\delta\theta/\delta x$ values were needed to develop a sea breeze in the presence of stronger positive u_G values (Fig. 8). Sea-breeze events associated with synoptic classes 4 and 6 were toward the lower-left corner of the diagram, in the region of strongly negative $\delta\theta/\delta x$ and weak or negative (landward) u_G. These events showed a tendency to be "early onset," but more detailed study at the mesoscale is required to resolve this question satisfactorily (Fig. 14). Sea-breeze events associated with classes 1 and 2 were confined to a relatively narrow diagonal region, running from the center-bottom boundary of the diagram (highly favorable $\delta\theta/\delta x$, and weak u_G) to the upper-left corner (unfavorable $\delta\theta/\delta x$, and near-zero or negative u_G) (Fig. 9), and sea-breeze events associated with class 6 were confined to an almost circular region in the upper-left part of the diagram (weakly favorable $\delta\theta/\delta x$, near-zero or negative u_G) (Fig. 13). Non-sea-breeze events associated with classes 2 and 3 were toward the upper-right corner of the diagram (highly unfavorable $\delta\theta/\delta x$, and strongly opposing u_G) (Fig. 9), with class 3 exhibiting the most extreme case, and non-sea-breeze events associated with class 5 were divided between a large circular region in the central part of the diagram (weakly favorable $\delta\theta/\delta x$, weak u_G), and a narrower area stretching from the center toward the lower-right corner (highly favorable $\delta\theta/\delta x$, but strongly opposing u_G) (Fig. 11).

The diagram (Fig. 8) is a useful tool for predicting sea-breeze events. Using the synoptic class, the sea surface temperature in the coastal zone (to act as a proxy for offshore air temperature), some idea of the daily temperature curve for some point well inland, and the magnitude of the cross-shore geostrophic wind component, one can decide—often with a high degree of confidence—whether or not a sea breeze will occur in the study area. This method is similar to one developed by Simpson (1994, chapter 4) for Thorney Island in the United Kingdom and is, in principle, adaptable to any coastal region of the world.

Acknowledgments. We thank Dr. Huiting Mao for contributing to this work. This research was conducted as part of Atmospheric Investigation, Regional Modeling, Analysis, and Prediction (AIRMAP), and is supported by NOAA Grants NA07RP0475 and NA17RP1488.

REFERENCES

Apel, J. R., 1987: *Principles of Ocean Physics.* Academic Press, 634 pp.

Barbato, J. P., 1975: The sea breeze of the Boston area and its effect on the urban atmosphere. Ph.D. dissertation, Boston University Graduate School, 223 pp.

Brown, W. S., and J. D. Irish, 1993: The annual variation of water mass structure in the Gulf of Maine: 1986–1987. *J. Mar. Res.,* **51,** 53–107.

Carnahan, B., H. A. Luther, and J. O. Wilkes, 1990: *Applied Numerical Methods.* Krieger, 604 pp.
Clark, W. A. V., and P. L. Hosking, 1986: *Statistical Methods for Geographers.* John Wiley and Sons, 518 pp.
Craig, R. A., I. Katz, and P. J. Harney, 1945: Sea–breeze cross sections from psychrometric measurements. *Bull. Amer. Meteor. Soc.,* **26,** 405–410.
Feng, H., 1996: Wind-induced responses of the western coastal Gulf of Maine during spring and summer, 1994. M.S. thesis, Dept. of Earth Sciences, University of New Hampshire, 104 pp.
Fisher, E. L., 1960: An observational study of the sea breeze. *J. Meteor.,* **17,** 645–660.
Frizolla, J. A., and E. L. Fisher, 1963: A series of sea breeze observations in the New York City area. *J. Appl. Meteor.,* **2,** 722–739.
Gaza, R. S., 1998: Mesoscale meteorology and high ozone in the northeast United States. *J. Appl. Meteor.,* **37,** 961–977.
Hsu, S. A., 1988: *Coastal Meteorology.* Academic Press, 260 pp.
Johnson, R., 1992: *Elementary Statistics.* PWS-Kent Publishing, 730 pp.
Kraus, H., J. M. Hacker, and J. Hartmann, 1990: An observational aircraft-based study of sea-breeze frontogenesis. *Bound.-Layer Meteor.,* **53,** 223–265.
Miller, J. E., 1948: On the concept of frontogenesis. *J. Meteor.,* **5,** 169–171.
Miller, S. T., 1999: Air–sea heat flux in the Gulf of Maine: Meteorological forcing and oceanic response. M.S. thesis, Dept. of Earth Sciences, University of New Hampshire, 232 pp.
Neumann, J., 1977: On the rotation of the direction of sea and land breezes. *J. Atmos. Sci.,* **34,** 1913–1917.
Pignotti, V., 1987: A meso-meteorological feature associated with high ozone concentrations in the northeastern United States. *J. Air Pollut. Control Assoc.,* **37,** 720–722.
Reible, D. D., J. E. Simpson, and P. F. Linden, 1993: The sea breeze and gravity-current frontogenesis. *Quart. J. Roy. Meteor. Soc.,* **119,** 1–16.
Seaman, N. L., and S. A. Michelson, 2000: Mesoscale meteorological structure of a high-ozone episode during the 1995 NARSTO-northeast study. *J. Appl. Meteor.,* **39,** 384–398.
Simpson, J. E., 1994: *Sea Breeze and Local Winds.* Cambridge University Press, 234 pp.
——, 1997: *Gravity Currents in the Environment and the Laboratory,* 2d ed. Cambridge University Press, 244 pp.
——, and P. F. Linden, 1989: Frontogenesis in a fluid with horizontal density gradients. *J. Fluid Mech.,* **22,** 1–16.
U.S. Air Force, 1998: Surface weather observations. Air Force Manual 15-111: U.S. Air Force, 113 pp. [Available online at http://afpubs.hq.af.mil/.]
U.S. Environmental Protection Agency, 1994: NARSTO research strategy and charter. U.S. EPA, 155 pp.
WMO, 1956: *International Cloud Atlas.* WMO 407, World Meteorological Organization, 156 pp.
Zhong, S., and E. S. Takle, 1993: The effects of large-scale winds on sea–land–breeze circulations in an area of complex coastal heating. *J. Appl. Meteor.,* **32,** 1181–1195.